"An algorithm to determine Paris Law constants evaluating crack sizes in aircraft fuselage panels using EKF"

A Project Report Submitted to
Gujarat Technological University in Partially Fulfilment of the Requirements for the Degree of Bachelor of Engineering
In
Information Technology

B. E. IV, Semester –VII

By

DhruvApte **Enrollment No. 150110119026**
Mohit Dhoriya **Enrollment No. 150110119065**

Faculty Guide

Prof.Nitinchandra Patel

Academic Year 2018-19

Department of Mechanical Engineering
G H Patel College of Engineering & Technology
VallabhVidyanagar, Anand

Acknowledgment

We appreciate the **GTU** for giving us a platform which can transform our idea into a design or any product which can help people in their day to day life.

We thank to our guide, **PROF. Nitinchandra Patel** (assistant Professor –ME)for their valuable guidance & the efforts that they have put in each of us. We would not have been able to complete our project without their cooperation, encouragement and immense help.

We are also thankful to other faculty members for their friendly advice and devoted instructions. A report is all-encompassing as this is never the work of one or two people labouring in quiet solitude. It is the product of many hands, and countless hours from many people. Our thanks go to all those who helped us.

DhruvApte
150110119026

Mohit Dhoriya
150110119065

COLLEGE CERTIFICATE

This is to certify that the project entitled "An algorithm to determine Paris Law constants evaluating cracksizes in aircraft fuselage panels using EKF" has been carried out by DhruvApte (150110119026) and Mohit Dhoriya (150110119065) under my guidance in partiallyfulfillment for the degree of Bachelor of Engineering in Information Technology (7th Semester) of Gujarat Technological University, Ahmedabad during the academic year 2018-19.

Internal Guide	Head of Department
Prof. Nitinchandra Patel Assistant Professor (ME)	Dr Darshak Desai Head & Professor (ME)

Seal of Institute

Undertaking of Originality of Work

We hereby certify that we are the sole authors of this UDP project report and that neither any part of this UDP project report nor the whole of the UDP project report has been submitted for a degree by other student(s) to any other University or Institution.

We certify that, to the best of our knowledge, the current UDP project report does not infringe upon anyone's copyright nor violate any proprietary rights and that any ideas, techniques, quotations or any other material from the work of other people included in our UDP project report, published or otherwise, are full acknowledged in accordance with the standard referencing practices. Furthermore, to extent that we have included copyrighted material that surpasses the boundary of fair dealing within the meaning of the Indian Copyright(Amendment) Act 2012, we certify that we have obtained a written permission from the copyright owner(s) to include such material(s) in the current UDP project report and have included copies of such copyright clearances to our appendix.

We declare that this is a true copy of our report, including any final revisions, as approved by our supervisors.

Date:

Place:

Team

Enrollment No.	Name	Signature
150110119026	Dhruv Apte	
150110119065	Mohit Dhoriya	

Index

List of Tables

Notation	
$\Delta\sigma$	Stress Range
N_f	Number of cycles to failure
a	Crack length
ΔK_t	Range of stress intensity factors
K_{th}	fatigue threshold
K_{tc}	fracture toughness with C and a being constants
^	Signifies that variable is estimated

Variable	Significance
^	Estimate
k	Time step
+	Prior estimate
-	Posterior estimate

ABSTRACT: The use of steel and aluminium alloys in making of aircraft components including fuselage, plates and flanges has increased since the post-WW II era. In the recent years, Aluminium 2024 has been extensively used in aircraft structures due to its high strength fatigue resistance, and due to the excessive weight of steel alloys. However, aluminium alloys also experience metal fatigue which results in accumulation of damage in the form of "cracks" due to repetitive application of loads. To study the dynamics of the failing system, Paris' Law has been found one of the most effective methods. But, there are uncertainties in the crack constants. To overcome this non-linearity, we have devised an algorithm using GNU Octave based on the Extended Kalman Filter. Our research is to determine the constants using EKF and analyse the crack sizes formed in a fuselage.

Keywords- Metal Fatigue, Paris's Law, Paris's Law constants Extended Kalman Filters (EKF)

INTRODUCTION

The concept of “fatigue" arose several times, as in the growth of cracks in the Comet aircraft that led to disaster when they became large enough to propagate catastrophically as predicted by the Griffith criterion. Fatigue, as understood by materials technologists, is a process in which damage accumulates due to the repetitive application of loads that may be well below the yield point. The process is dangerous because a single application of the load would not produce any ill effects, and a conventional stress analysis might lead to a assumption of safety that does not exist. In one popular view of fatigue in metals, the fatigue process is thought to begin at an internal or surface f aw where the stresses are concentrated, and consists initially of shear flow along slip planes. Over a number of cycles, this slip generates intrusions and extrusions that begin to resemble a crack. A true crack running inward from an intrusion region may propagate initially along one of the original slip planes, but eventually turns to propagate transversely to the principal normal stress as seen in Fig. 1.

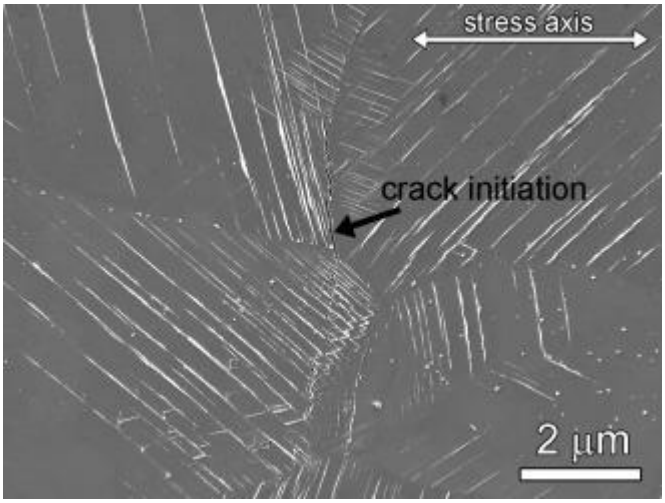

Figure 1: Intrusion-extrusion model of fatigue crack initiation.

When the failure surface of a fatigued specimen is examined, a region of slow crack growth is usually evident in the form of a “clamshell" concentric around the location of the initial f aw. (See Fig. 2.) The clamshell region often contains concentric “beach marks" at which the crack was arrested for some number of cycles before resuming its growth. Eventually, the crack may become large enough to satisfy the energy or stress intensity criteria for rapid propagation, following the previous expressions for fracture mechanics. This final phase produces the rough surface typical of fast fracture. In post-mortem examination of failed parts, it is often possible to correlate the beach marks with specific instances of overstress, and to estimate the applied stress at failure from the size of the crack just before rapid propagation and the fracture toughness of the material.

Figure 2: : Typical fatigue-failure surfaces. From B. Chalmers, Physical Metallurgy, Wiley, p. 212, 1959.

S-N curves

Well before a microstructural understanding of fatigue processes was developed, engineers had developed empirical means of quantifying the fatigue process and designing against it. Perhaps the most important concept is the S-N diagram, such as those shown in Fig. 41, in which a N is applied to a specimen and the number of loading cycles Σconstant cyclic stress amplitude until the specimen fails is determined. Millions of cycles might be required to cause failure at lower loading levels, so the abscissa in usually plotted logarithmically.

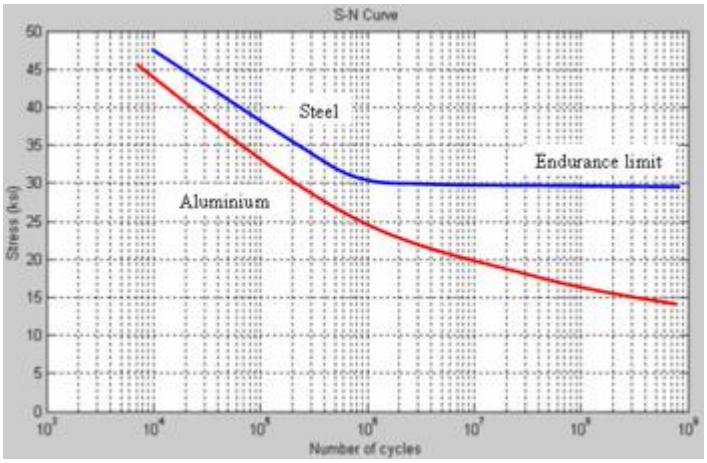

Figure 3: S-N diagrams for Aluminium and Low Carbon Steel

In some materials, notably ferrous alloys, the − curve flattens out eventually, so that below a certain endurance limit failure does not occur no matter how long the loads are cycled. Obviously, the designer will size the structure to keep the stresses below by a suitable safety factor if cyclic loads are to be withstood. For some other materials such as aluminium, no endurance limit exists and the designer must arrange for the planned lifetime of the structure to be less than the failure point on the − curve.

Statistical variability is troublesome in fatigue testing; it is necessary to measure the lifetimes of perhaps twenty specimens at each of ten or so load levels to de ne the − curve with statistical con dence[2]. It is generally impossible to cycle the specimen at more than approximately 10Hz (inertia in components of the testing machine and heating of the specimen often become problematic at higher speeds) and at that speed it takes 11.6 days

to reach 10^7 cycles of loading. Obtaining a full − curve is obviously a tedious and expensive procedure.

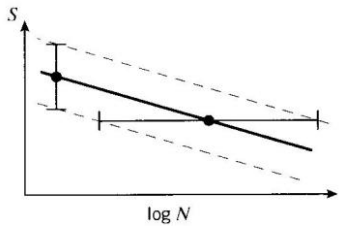

Figure 4: Variability in fatigue lifetimes and fracture strengths

LITERATURE REVIEW

The concept of metal fatigue was not worked well upon in aerodynamic designs, until 1954 when two de Havilland Comets broke up in mid-air within few months. A Court of Inquiry was set up by the British government to investigate the causes. Titled as the Cohen Committee after its chairman Lord Cohen, it ultimately published a report citing metal fatigue as the main cause. The stress concentration caused by stress generation near the windows was nearly three times the stress experienced around the fuselage. The planes were immediately grounded and aerospace firms were instructed to make round-shaped windows instead of the previously square-shaped ones.

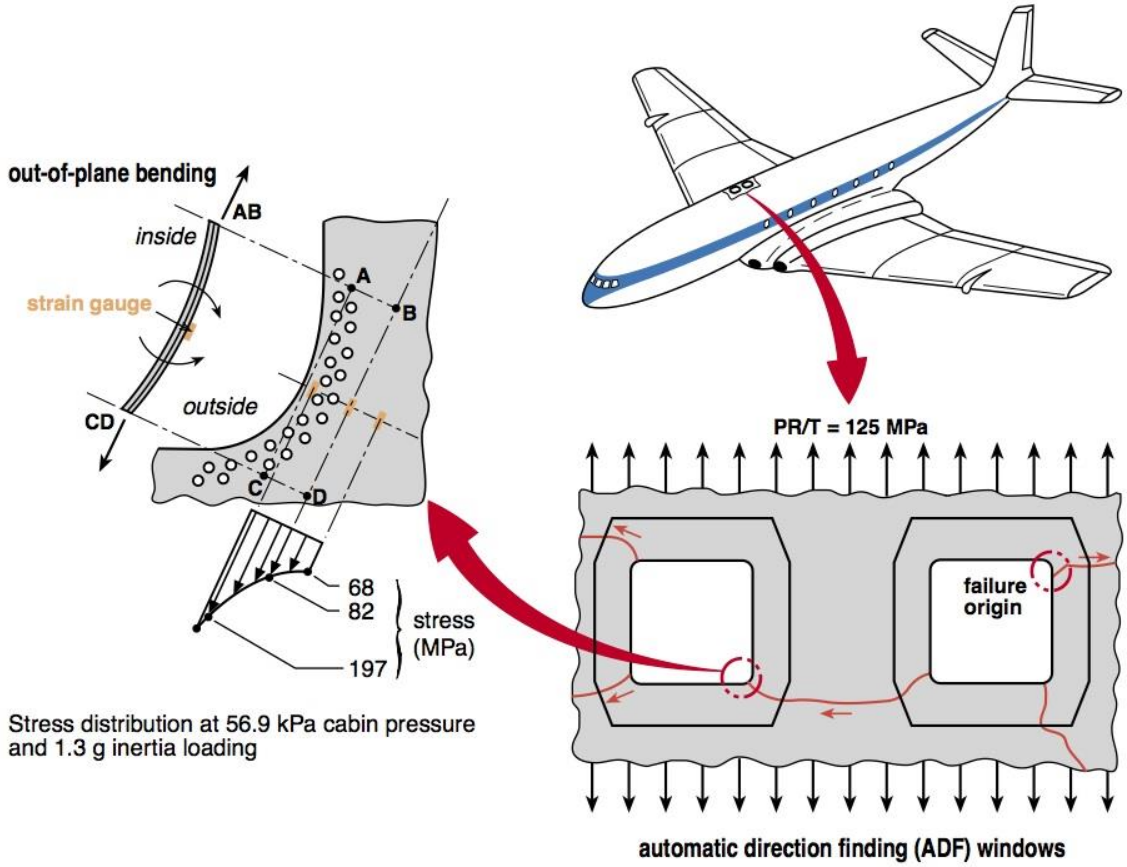

Figure 5: Failure origin of Comet G-ALYU around square windows (Source: Aerospace Engineering Blog)

Not only windows, but fuselage panels too have been developing flaw sizes resulting sometimes in deadly disasters.

Figure 5: Damaged fuselage part of a Southwest 737-300 plane while airborne as a result of cyclic stresses (Source: Seattle Times)

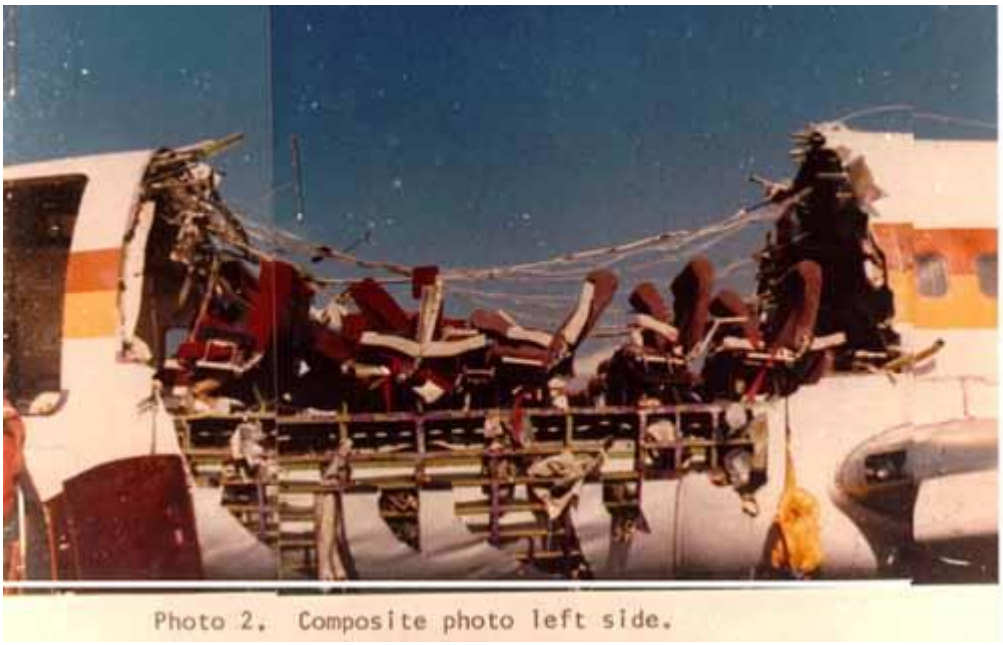

Figure 6: Aloha Airlines Flight 243; a huge part of fuselage about 5.6 m ruptured while airborne resulting in a casualty. Air crash investigation pointed the cause to fatigue and poor maintenance by the airline. (Part of subsequent case study)

The fatigue process is thought to begin at a surface flaw where stress concentrations occur. It consists of shear flow along slip planes which generate extrusions over a number of cycles, eventually forming a crack. During examination, a region of slow crack growth is observed in the form of a “clamshell” that is concentric around location of the initial flaw. In post-mortem examinations, it is possible to relate the “clamshell” to the initial stress and determine the applied stress at failure just before crack propagation.

Previously, engineers had developed quantification of fatigue with empirical formulae. The first model was the S-N curve where constant cyclic stress amplitude is applied to a specimen and number of loading cycles N when the specimen fails is determined. For materials like aluminium, no endurance limit exists. Although, in use in industry, obtaining a full S-N curve

is a tedious and expensive process. This problem was solved by Basquin in 1910 when he proposed a law later known as Basquin's Law:

$$\Delta\sigma N_f^a = C$$

Where Δσ is stress range, N_f is number of cycles to failure, a & C are empirically determined constants.

Crack growth will accelerate over life of the airplane part. This was the main shortcoming of the Miner's Law. The Miner's Law states that where there are *k* different stress magnitude values in a spectrum S_i ($1 \leq i \leq k$), each contributing n_iS_i cycles then if N_iS_i is the number of cycles to failure of a constant stress reversal S_i , failure occurs when:

$$\Sigma \frac{n_i}{N_i} = C$$

For design purposes, C is assumed to be 1.

Damage accumulation is a combination of several different mechanisms and the Miner's Law assumes only linear damage accumulation. Though this might make calculations easy, this will not be practically correct as when fatigue progresses, parts of the material microstructure become unable to bear the load which increases the stress on the surviving microstructure elements, thus increasing the rate of damage in the final portions of its lifetime.

Fatigue initiation and crack growth has lead to two design approaches for aircraft design: damage tolerant design and safe life design; the latter being lesser used.

An aircraft always has small cracks and there is no cause of worry in it. It is only when they reach a critical size that the consequences are lethal. In aviation slang, a crack reaches critical size when it grows large enough to 'let go' under operating loads. To find accurate crack size, in 1961, P.C. Paris introduced a formula that explained the relationship between crack growth rate during cyclic loading and stress intensity factor on a log-log graph; the details of which are explained in the nest section.

CASE STUDIES

CASE STUDY 1: JAPAN AIRLINES FLIGHT 123

Japan Airlines Flight 123 was a scheduled domestic Japan Airlines passenger flight from Tokyo's Haneda Airport to Osaka International Airport, Japan. On Monday, August 12, 1985, a Boeing 747SR operating this route suffered a sudden decompression twelve minutes into the flight and crashed in the area of Mount Takamagahara, Ueno, Gunma Prefecture, 100 kilometres (62 miles) from Tokyo thirty-two minutes later. The crash site was on Osutaka Ridge, near Mount Osutaka. The crash is the deadliest single aircraft disaster in aviation history killing 505 of the 509 passengers and all the 15 crew.

Figure 7: Correct and Incorrect splice plate installations

Cause of Crash

1. The aircraft was involved in a tail strike incident at Osaka International Airport seven years earlier as JAL Flight 115, which damaged the aircraft's rear pressure bulkhead.
2. The subsequent repair of the bulkhead did not conform to Boeing's approved repair methods. For reinforcing a damaged bulkhead, Boeing's correct repair calls for one continuous splice plate with three rows of rivets. However, according to the Federal

Aviation Administration, the Boeing technicians carrying out the repair had cut the plate specified for the job into two pieces parallel to the stress crack it was intended to reinforce, "to make it fit."]Cutting the plate in this manner negated the effectiveness of one of the rows of rivets, reducing the part's resistance to fatigue cracking to about 70% of that for a correct repair. During the investigation, Boeing calculated that this incorrect installation would fail after approximately 10,000 pressurization cycles; the aircraft accomplished 12,318 successful flights from the time that the faulty repair was made to when the crash happened.

3. Consequently, after repeated pressurization cycles during normal flight, the bulkhead gradually started to crack near the single row of rivets holding it together. When it finally failed, the resulting rapid decompression ruptured the lines of all four hydraulic systems and ejected the vertical stabilizer. With many of the aircraft's flight controls disabled, the aircraft became uncontrollable.

CASE STUDY 2: ALOHA AIRLINES FLIGHT 243

Aloha Airlines Flight 243 was a scheduled Aloha Airlines flight between Hilo and Honolulu in Hawaii. On April 28, 1988, a Boeing 737-297 serving the flight suffered extensive damage after an explosive decompression in flight, but was able to land safely at Kahului Airport on Maui. There was one fatality, flight attendant Clarabelle Lansing, who was ejected from the airplane. Another 65 passengers and crew were injured. Despite the substantial damage inflicted by the decompression, and the loss of one cabin crew member, the safe landing of the aircraft established the incident as a significant event in the history of aviation, with far-reaching effects on aviation safety policies and procedures. While the airframe had only accumulated 35,496 flight hours prior to the accident, those hours were over 89,680 flight cycles (a flight cycle is defined as a takeoff and a landing), owing to its use on short flights.

Figure 8: A pictorial explanation of how a small fatigue crack resulted in the rupture of a huge section of the fuselage.

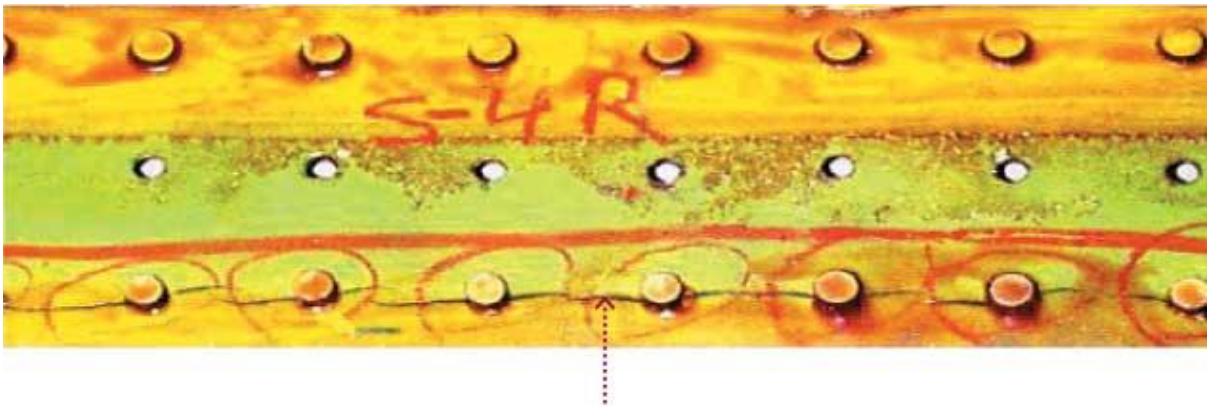

Figure 9: Crack marked in red. The crack spread through riveting joints in the stiffener as these were points of high stress concentration.

Causes of crash

For the aircraft production number 292 (B-737) and after (this aircraft was production line number 152), an additional outer layer of skin or doubler sheet at the lap joint of the fuselage was added. In the construction of this aircraft this doubler sheet was not used in addition to other details of the bonding of the parts. In the case of production line 292 and after, this doubler sheet gave an additional thickness of 0.91 mm (0.036 in) at the lap joint. In airplane line number 291 and before, cold bonding had been utilized, with fasteners used to maintain surface contact in the joint, allowing bonding adhesive to transfer load within the joint. This cold bonded joint used an epoxy-impregnated woven scrim cloth to join the edges of 0.9 mm thick skin panels. These epoxy cloths were reactive at room temperature, so they were stored at dry ice temperatures until used in manufacture. The bond cured at room temperature after assembly. The cold bonding process reduced the overall weight and manufacturing cost. Fuselage hoop loads (circumferential loads within the skins due to pressurization of the cabin) were intended to be transferred through the bonded joint, rather than through the rivets, allowing the use of lighter, thinner fuselage skin panels with no degradation in fatigue life.

The additional outer layer construction improved the joint by:

- Eliminating the knife-edge fatigue detail, which resulted from the countersinking of the panels for flush rivets in a disbonded upper skin;
- Eliminating the corrosion concern associated with the scrim cloth, which could wick moisture into the lap joint

The investigation determined that the quality of inspection and maintenance programs was deficient. As fuselage examinations were scheduled during the night, this made it more difficult to carry out an adequate inspection of the aircraft's outer skin.

Also, the fuselage failure initiated in the lap joint along S-10L; the failure mechanism was a result of multiple site fatigue cracking of the skin adjacent to rivet holes along the lap joint upper rivet row and tear strap disbond, which negated the fail-safe characteristics of the fuselage. Finally, the fatigue cracking initiated from the knife edge associated with the countersunk lap joint rivet holes; the knife edge concentrated stresses that were transferred through the rivets because of lap joint disbonding.

The NTSB concluded in its final report on the accident:

“The National Transportation Safety Board determines that the probable cause of this accident was the failure of the Aloha Airlines maintenance program to detect the presence of significant disbonding and fatigue damage which ultimately led to failure of the lap joint at S-10L and the separation of the fuselage upper lobe. Contributing to the accident were the failure of Aloha Airlines management to supervise properly its maintenance force; the failure of the FAA to require Airworthiness Directive 87-21-08 inspection of all the lap joints proposed by Boeing Alert Service Bulletin SB 737-53A1039; and the lack of a complete terminating action (neither generated by Boeing nor required by the FAA) after the discovery of early production difficulties in the B-737 cold bond lap joint which resulted in low bond durability, corrosion, and premature fatigue cracking.”

PARIS' LAW

Certainly in aircraft, but also in other structures as well, it is vital that engineers be able to predict the rate of crack growth during load cycling, so that the part in question be replaced or repaired before the crack reaches a critical length. A great deal of experimental evidence supports the view that the crack growth rate can be correlated with the cyclic variation in the stress intensity factor:

$$\frac{da}{dN} = A(\Delta K_t^m)$$

Here A and m are constants that depend on the material, environment and stress ratio.

What made the Paris Law different from S-N curve was that it took considerably different components than the latter. This caused slower damage propagation in uncracked surfaces which was expected. The Paris Law's long crack propagation theory further implied that the dependence on the initial size of the crack was different from that calculated by crack propagation threshold and toughness value. The law often gives fairly accurate results and which may be termed as 'beautiful'. But when it does not work, it gives a serious limitation of having stress intensity factor on the x-axis. If the factor range cannot correctly predict the crack, we are left with a multivariate function with sparse data points making it more difficult for analysis.

Scientists have therefore modified the Paris Law and published the variations. These variations include only a single factor removal or departure from the ideal conditions. Modifications worth mentioning in this paper include crack closure (Elber, 1970) and short cracks (Richie and Lankford, 1986, 1996; El Hadad et al., 1979; Kitahaka and Tanaka, 1990).

The Paris Law as modified by Paris and Erdogan in 1963 gives the advancement of fatigue crack per unit cycle as a function of the stress intensity factor:

$$v^a = \frac{da}{dN} = C\Delta K^m, \Delta K_{th} < \Delta K < K_{tc}$$

Where K_{th} = fatigue threshold

K_{tc} = fracture toughness with C and a being constants

CRACK GROWTH MODEL

Consider an infinite elastic plate with symmetric crack of length 2a. Here the stress intensity factor can be represented as:

$$K = \sigma\sqrt{\pi a}$$

By integrating, we get:

$$K^* = \sigma\sqrt{\pi(a + \frac{\Delta a}{2})}$$

Although the crack propagation is a continuous process, a discrete process can measure the size of the crack after every flight cycle. The reason for a non-continuous algorithm is that perhaps the EKF algorithm might not be computationally correct in integrating the system dynamics for a continuous system.

Thus the Paris's law equation for each flight cycle *k* in a recursive format can be written as:

$$a_k = a_{k-1} + C(\frac{p_{k-1}r}{t}\sqrt{\pi a_{k-1}})^m$$

$= g(a_{k-1}, p_{k-1})$ .....(1)

We will use this equation during the parameter estimation and designing of the algorithm.

Since *m* and *C* are the parameters that depend on the material properties and remain constant, we only have *p* varying at every flight cycle. The pressure p_k can be expressed as:

$$p_k = \bar{p} + \Delta p_k$$

The Δp_k is regarded as a disturbance and is modelled as a centred normal distribution with variance σ^2. We will model this using a perturbation term.

Modifying equation (1),

$$a_k = g(a_{k-1}, \bar{p} + \Delta p_{k-1})$$

The indices produced by each mechanically performed function should be the same irrespective of method of evaluation. Wang (2016) have used the Mean Value First Order Second Moment (MVFOSM) approach but, in some cases the approach does not support the above condition. Hence this paper will consider using the second order Taylor expression

$$a_k = g(a_{k-1}, \bar{p}) + \frac{\partial g(a_{k-1}, \bar{p})}{\partial p}\Delta p_{k-1} + \frac{1}{2}\frac{\partial^2 g(a_{k-1}, \bar{p})}{\partial p^2}\Delta p_{k-1}$$

Where $\frac{\partial g(a_{k-1}, \bar{p})}{\partial p}\Delta p_{k-1}$ and $\frac{\partial^2 g(a_{k-1}, \bar{p})}{\partial p^2}\Delta p_{k-1}$ are first order and second order partial derivatives of *g* with respect to variable *p* at the point $(a_{k-1}, \bar{p})$.

$$\frac{\partial g(a_{k-1}, \bar{p})}{\partial p} = Cm({}^{r}/_{t}\sqrt{\tau a_k})^m(\bar{p})^{m-1}$$

$$\frac{\partial^2 g(a_{k-1},\bar{p})}{\partial p^2} = Cm(m-1)({}^{r}/_{t}\sqrt{\tau a_k})^m(\bar{p})^{m-2}$$

Taking the above two derivatives as addictive noise w_{k-1} and considering $\bar{p}$ as a given constant, the equation can be written as:

$$a_k = f(a_{k-1}) + w_{k-1}$$

The additive process noise w_k is assumed to be zero mean additive white Gaussian noise i.e.

- Interpreted as the sum of two components: a noise-free component and the noise component (additive).
- The noise component is random but it is assumed that it is drawn at each sample time from a fixed Gaussian distribution.
- White signifies the noise signal containing same power samples at equal frequencies.

This noise is now defined as Q_k:

$$Q_k = \left[\frac{\partial g(a_{k-1},\bar{p})}{\partial p} + \frac{\partial^2 g(a_{k-1},\bar{p})}{\partial p^2}\right]^2$$

$$Q_k = Cm({}^{r}/_{t}\sqrt{\pi a_k})^m(\bar{p})^{m-1}\left[1 + \frac{m-1}{\bar{p}}\right]$$

The measurement data is stated since crack size measured by sensors will always contain noise from measurement environment and instrument inaccuracies, how small the latter might be.

$$z_k = h(a_k) + v_k$$

Where h is measurement function and v_k is the noise. Thus the system and measurement equations are defined.

EXTENDED KALMAN FILTER

The extended Kalman filter is regarded as technique that uses Kalman filter as a base for non-linear function. The filter allows state transition and observation models to be differentiable functions.

$$x_k = f(x_{k-1}, u_k) + w_k$$

$$z_k = h(x_k) + v_k$$

Where w_k and v_k are the process and observation noises with covariance as W_k and V_k respectively and u_k is the control vector.

To explain the equations in words, the function f predicts the state from given estimate and the function h predicts the measurement from the former. Then the Jacobian function is computed.

The papers published by Swirling (1958), Kalman (1960) and Kalman & Bucy(1961) unified the above equations as:

$$\hat{x}_k = \hat{x}_{k-1} + k_k(z_k - \hat{x}_{k-1})$$

Where the carat '^' signifies that the variable is estimated. The variable k is known as the Kalman gain.

PROBLEM FORMULATION

Parameter estimation can either be done using joint filtering or dual filtering. For the sake of simplicity, we have used joint filtering here for joint estimation of Paris's Law material properties and crack size. We define the parameter vector of interest as the additional state variable and then add it to the true state vector. This appended part remains constant during the process noise while the error covariance matrix is propagated as a whole.

Estimation framework

The parameters that are needed to be estimated are m and C. We will now define a two dimensional parameter vector as:

$$\theta = [m, C]^T$$

Appending crack length, *a:*

$$x_{aug} = [a \quad m \quad C]^T$$

We will be using the subscript, "*aug*" for denoting the augmented variables. The extended system can now be expressed in terms of a matrix as:

$$x_{aug,k} = f_{aug}(x_{aug,k-1}) + w_{aug,k-1}$$

$$\begin{bmatrix} a_k \\ m_k \\ C_k \end{bmatrix} = \begin{bmatrix} f(a_{k-1}) \\ m_{k-1} \\ C_{k-1} \end{bmatrix} + \begin{bmatrix} w_{k-1} \\ 0 \\ 0 \end{bmatrix}$$

The augmented process noise covariance matrix can be expressed in the form of

$$Q_{aug,k} = \begin{bmatrix} Q_k & 0 & 0 \\ 0 & 0 & 0 \\ 0 & 0 & 0 \end{bmatrix}$$

The measurement equation should also be expanded as the following:

$$z_{aug,k} = h_{aug}(x_{aug,k}) + v_{aug,k}$$

$$\begin{bmatrix} z_{a,k} \\ z_{m,k} \\ z_{C,k} \end{bmatrix} = \begin{bmatrix} a_k \\ m_k \\ C_k \end{bmatrix} + \begin{bmatrix} v_{a,k} \\ v_{m,k} \\ v_{C,k} \end{bmatrix}$$

The '*v*' variables represent the measurement noise of the constants. Since it is a white Gaussian noise, the noise of each state will have zero mean and variance of R_a, R_m, R_C.

RELEVANT MATLAB CODE

```
function [X] = flawsize( K,T,C,t,f)

%FLAWSIZE Summary of this function goes here

%   Detailed explanation goes here

% We will be investigating and predicting the flaw size of steel plates in an aircraft with a given lifespan

% Here K is fracture toughness

% T is the tensile load while C is compressive load

% t is the time limit of the aircraft(in years)

% f is the frequency at which stress is applied per minutes

% Using Paris Law

ac = ((K/(1*T))^2)/pi ;

%  Where Y is a geometry constant normally taken as 1

%  Calculating the number of cycles per year (N)

N = f*60*24*365*t;

% Applying modified equation of Paris Law

a = (exp((log((((N*(-1.2)*1.62*(10^-12)*(T^3.2)*(pi^1.6))/2)- (ac^(-0.6)))*(-1)))/(-0.6)))*1000

% where n and C are constant wiht value n=3.2 and C= 1.62*(10^-12)

X= ['The initial flaw size in mm will thus be ',num2str(a)];

disp(X);

end
```

FUTURE SCOPE

We will continue the algorithm building in the next semester. Right now, we have initialised the state parameters and derived it mathematically but it needs to be coded and computed. We also need to verify the findings of the algorithm with manual calculations and experimental findings to further make the fact concrete that the algorithm is accurate.

We have extended the Taylor series to the second differential. We can extend it to the third to see the result. However, as we increase the order of differential the order of accuracy becomes more and more less until there is virtually no change in accuracy. Thus, for calculation purposes have to limit it to a certain differential order.

We also will try to optimize the algorithm. The algorithm dependency on several variables makes it unstable in case even if a single algorithm is not known. Thus variables can be reduced to increase its stability.

We would discuss this algorithm with potential customers like aerospace companies like Boeing, Embraer and Honeywell Aerospace for their feedback. Their feedback and suggestions will surely improve the quality of research done to devise this algorithm.

REFERENCES

1. N. Pugno et. Al , A generalized Paris' law for fatigue crack growth, Journal of Mechanics and Physics of solids, 54(7):1333-1349 · July 2006
2. R. Branco et al , Determination of Paris law constants with a reverse engineering technique , Journal of Failure Mechanics 16 (2), 631-638
3. Yiwei Wang et al , Determination of Paris' law constants and crack length evolution via Extended and Unscented Kalman filter: An application to aircraft fuselage panels , Mechanical Systems and Signal Processing. Volume 80, 1 December 2016, Pages 262-281
4. Simon J. Julier et al , New extension of the Kalman filter to nonlinear systems , Society of Photo-Optical Instrumentation Engineers.
5. Chen d. et al, Bulging of fatigue cracks in a pressurized aircraft fuselage , Aeronautical fatigue: Key to safety and structural integrity. 1991 (A93-13626 02-39), p. 277-315.
6. J.R. Mohanty, B.B. Verma, P.K. Ray, Prediction of fatigue crack growth and residual life using an exponential model: Part I (constant amplitude loading), Int. J. Fatigue,
7. M. Yazdanipour et al , Stochastic fatigue crack growth analysis of metallic structures under multiple thermal–mechanical stress levels
8. M.C. Vandyke et al, Unscented Kalman fIltering for Spacecraft Attitude State and Parameter Estimation, The American Astronautical Society
9. G. Chowdhary, R. Jategaonkar, Aerodynamics parameter estimation from flight data applying extended and unscented Kalman filter, Aerosp. Sci. Technol.

CANVASES

AEIOU Summary

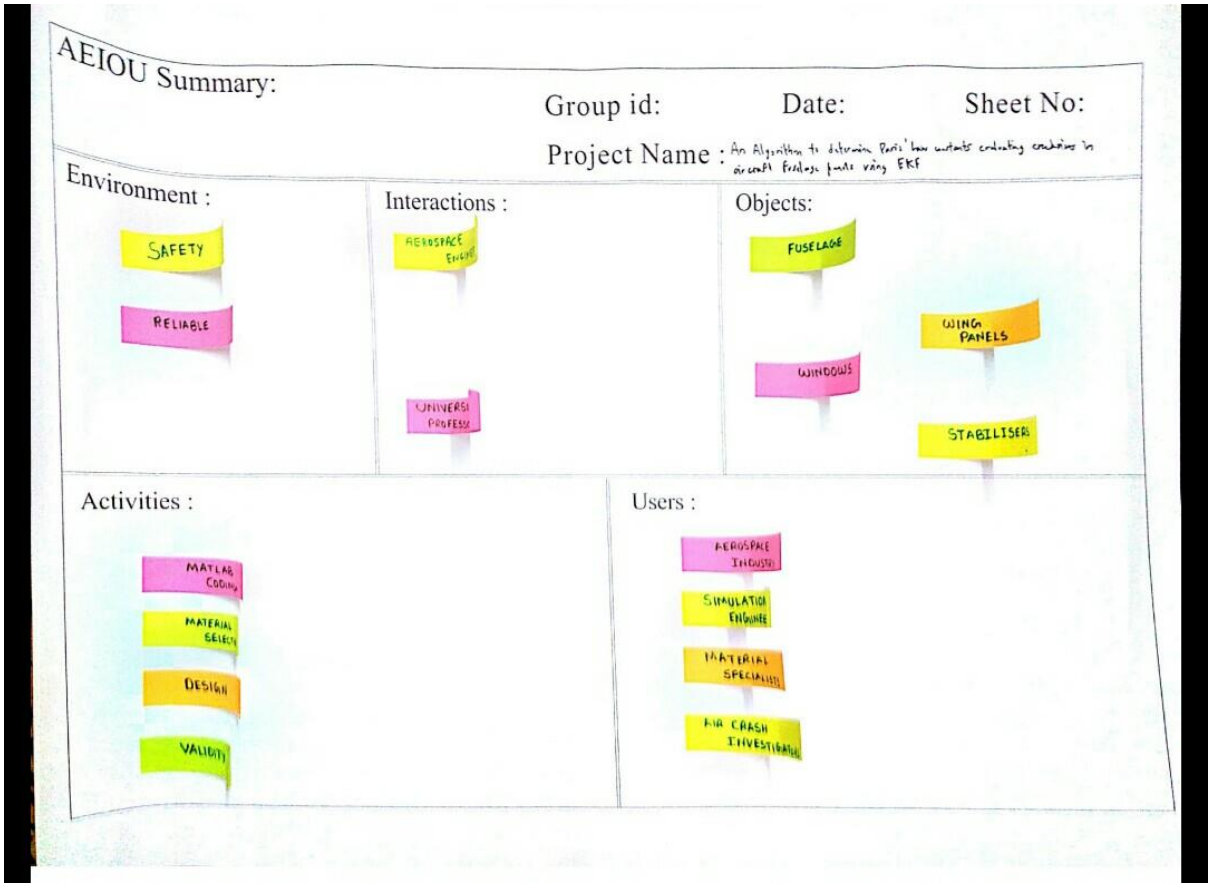

The above canvas is an AEIOU Summary about the Activities, Environment, Interactions, Objects and Users. Based on the observations done we were able to draft this summary which includes the situations and the major/minor factors that are responsible for the inactions

Product Development Canvas

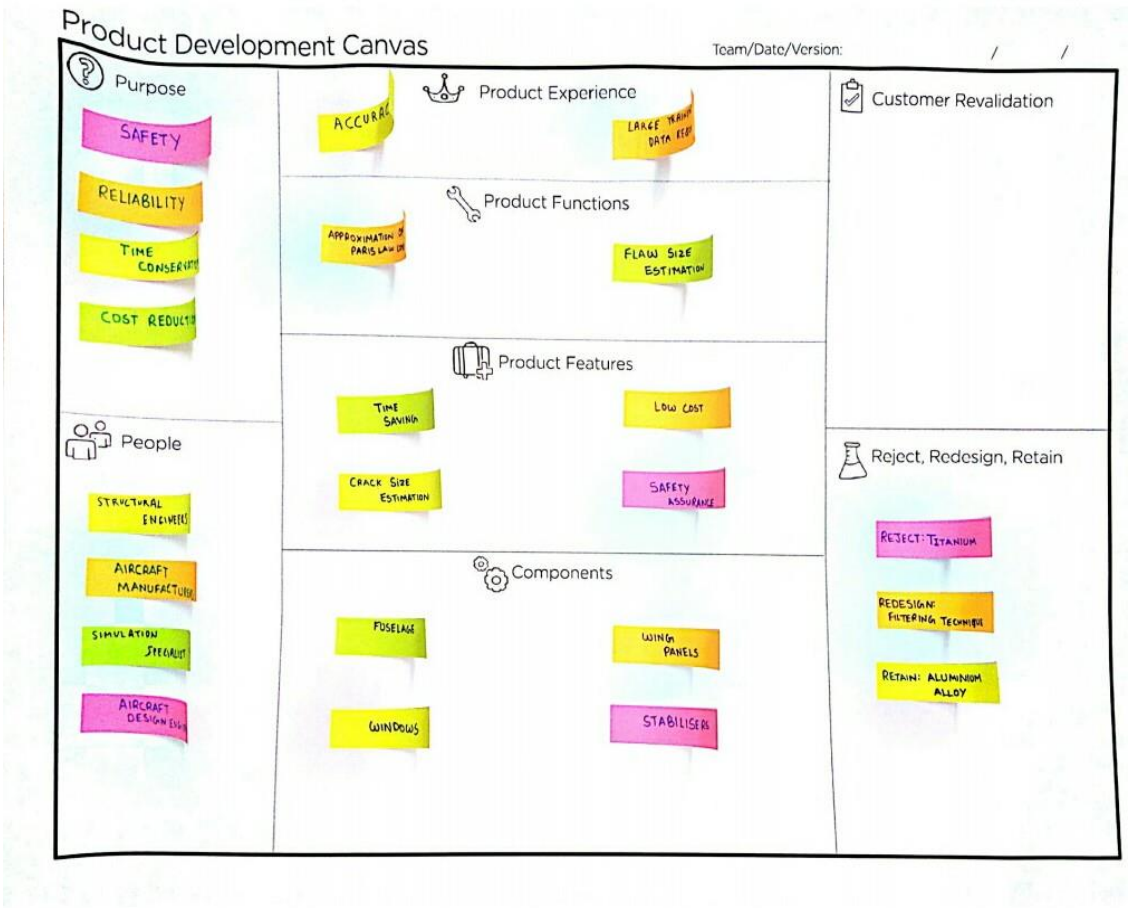

Based on the observation in the previous AEIOU summary a particular Ideation can be derived which results into the Ideation Canvas above. This canvas shows the initial idea about the formation of the product and shows that how a particular product should be designed. The factors that will be affecting the development of the product are also included in this canvas.

Empathy Summary

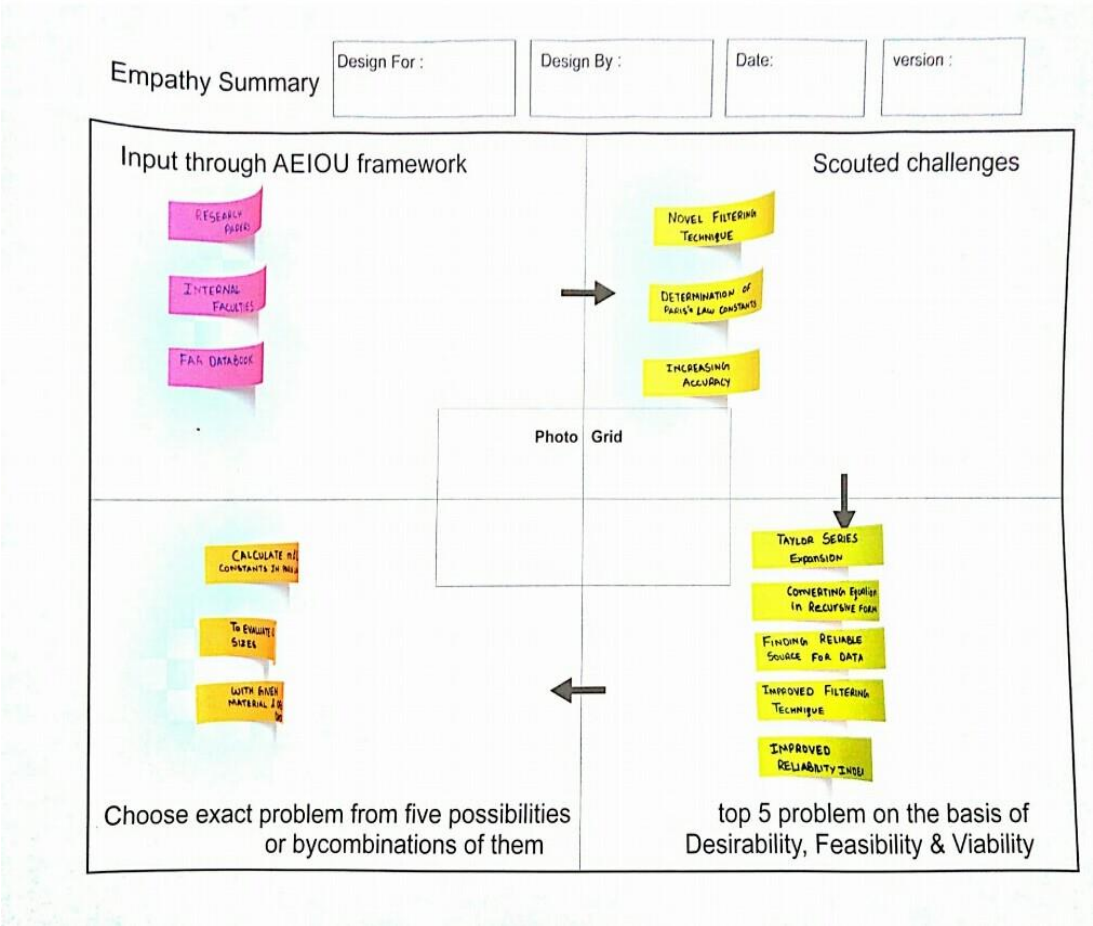

Ideation Canvas

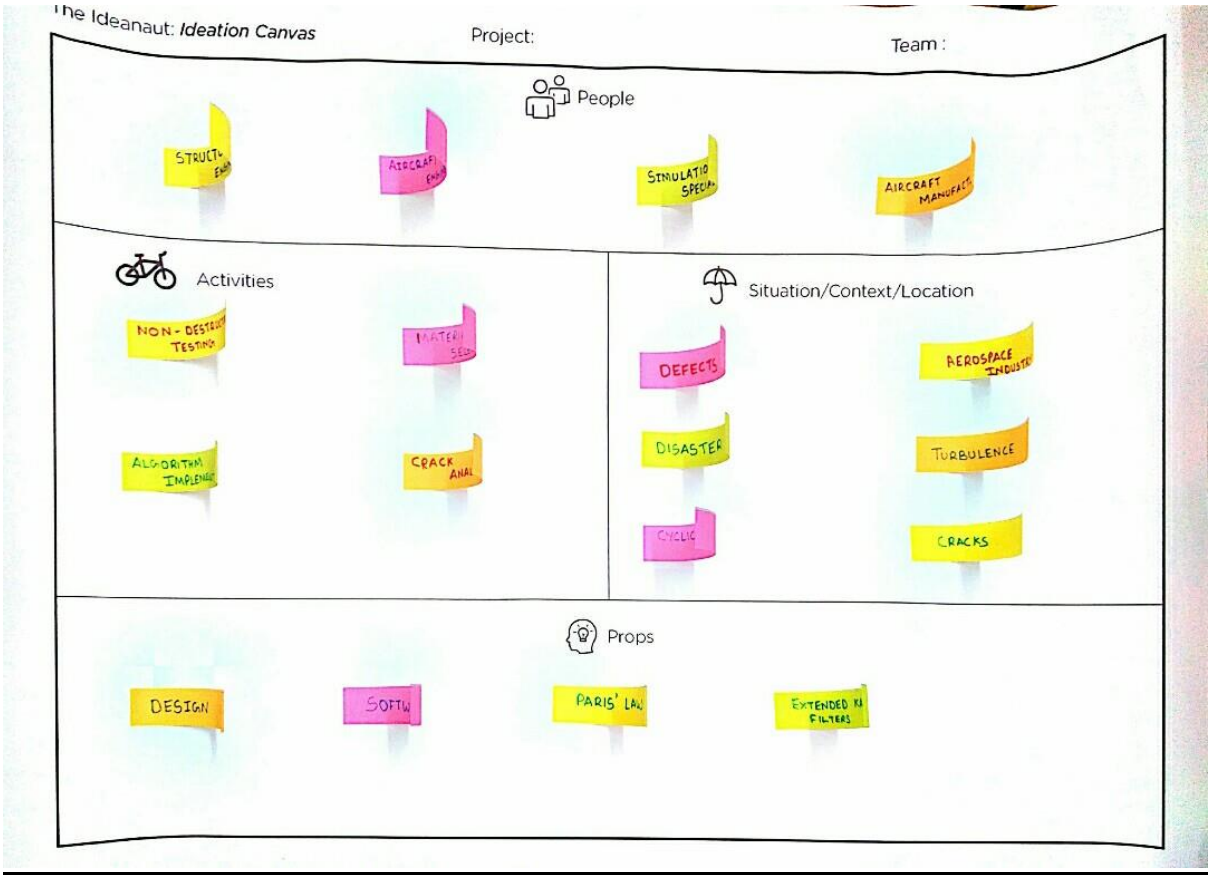

After understanding the ideal stage of the product and going through the empathy part of the product it is time to design the final product definition, users, features, functions and components. This canvas will let us know exactly the amount of efforts and the clear idea that is to be put into this project. After that, the Customer revalidation part shows us how true we were in idealizing and creating a solution for the user. After that according to the Validations it is up to us that we reject, redesign and retain the function and features according to the feedback from the customer.